Lightweight Alkali-Activated Material from Mining and Glass Waste by Chemical and Physical Foaming

Gediminas Kastiukas[1], Ph.D., Xiangming Zhou[2*], Ph.D., Kai Tai Wan[3], Ph.D. and João Castro Gomes[4], Ph.D.

[1]Research Fellow, Department of Civil and Environmental Engineering, Brunel University London, Uxbridge, Middlesex UB8 3PH, United Kingdom

[2]Professor, Department of Civil and Environmental Engineering, Brunel University London, Uxbridge, Middlesex UB8 3PH, United Kingdom (http://orcid.org/0000-0001-7977-0718)

[3]Lecturer, Department of Civil and Environmental Engineering, Brunel University London, Uxbridge, Middlesex UB8 3PH, United Kingdom

[4]Professor, Centre of Materials and Building Technologies, University of Beira Interior, 6200 Covilhã, Portugal (http://orcid.org/0000-0002-2694-5462)

([*]Corresponding author) e-mail: Xiangming.Zhou@brunel.ac.uk

ABSTRACT

A foamed alkali-activated material (FAAM), based on tungsten mining waste (TMW) and municipal waste glass (WG) was fabricated by using aluminium powder and organic surfactant foaming agents. The compressive strength and density of the FAAM were investigated in terms of different parameters of production and formulation including curing temperature as well as the dosage of Na_2O, foaming agent, foam catalyzing agent and stabilizing agent. FAAM made with aluminium powder consisted of smaller open macropores and exhibited higher compressive strength in comparison with those of larger closed macropores obtained by the organic surfactant counterparts. The final aluminium powder based FAAM reached a 7-day compressive strength in excess of 3 MPa and a density below 0.7 g/cm^3. The implementation of an appropriate amount of foam stabilizer led to a further 15% increase in compressive strength, 6% reduction in density and a thermal conductivity below 0.1 W/mK. The FAAM explored in this study represents an ideal material for building envelop insulation.

Keywords: Alkali-activation; aluminium powder; compressive strength; foamed cementitious materials; geopolymer; waste glass; waste materials

1. Introduction

The development and application of lightweight cementitious materials have in the past decades grown very rapidly and such materials are among the leading technology in the “special purpose” concrete category [1]. Autoclaved aerated concrete (AAC) is primarily used for making lightweight blocks to build partition walls. The lightweight nature of the blocks means that they impose a minimum loading on the building and provide good thermal and sound insulation [2]. Pre-fabricated panels can also be made from lightweight cementitious materials with the latest innovation being hollow-core, interlocking panels [3]. Another useful application of lightweight cementitious materials is void filling for structural stabilisation of disused structures [4].

Approximately 70% of heat energy is lost through the building envelope from typical residential housing without proper thermal insulation [5], making building insulation one of the fastest growing applications of lightweight cementitious materials [4].

The industry has been working hard to develop eco-friendly and energy efficient construction materials due to the increase in market demand. With the exception of organic insulation materials, which are based on a renewable and recyclable material, polymer-based insulation materials are associated with a host of environmental hazards in terms of toxicity. Polymer foam materials such as polystyrene and polyethylene remain very popular materials for insulation and make up almost half of the market [6]. Polystyrene is classified as a possible human carcinogen [7], and the production of Expanded Polystyrene Foam (EPS) has a global warming potential (GWP) 7 times greater than carbon dioxide [8]. Hence, the use of lightweight cementitious materials can constitute an effective way of energy-conservation and environmental-protection, particularly for the thermal-insulation engineering of buildings.

Currently, technologies for insulating performance are being explored, like aerogels [9] and Vacuum Insulating Panels (VIPs) [10]. However, these cannot be produced in a cost-effective manner and are too fragile to meet the durability needs that are critical for mainstream building products (e.g. VIPs cannot be nailed, and lose thermal resistance rapidly if perforated), making them impractical solutions for today's building environment.

There were several recent studies about lightweight foamed alkali-activated materials (AAM), which are referred to as geopolymers in some literature as well, based on fly ash [11] and bottom ash [12]. AAMs have been demonstrated to possess many of the necessary qualities a lightweight cementitious material should display, namely high temperature resistance [13], low shrinkage [14], low coefficient of permeability [15], low thermal conductivity [16] and good nailability [17]. Also, the appeal of being able to use high volumes of industrial waste materials for the production of AAMs and thus contest the environmental pollution of Portland cement is an added benefit.

So far, in building applications, the research into foamed alkali-activated materials (FAAMs) is limited to structural grade concrete with mid-range densities of 1300-1700 kg/m^3 and compressive strengths of 13-15 MPa [13], [18]–[20]. Out of the few studies conducted to produce high-performance FAAMs, the resulting materials possessed either high insulating properties coupled with very low compressive strength [21] or high compressive strength coupled with poor thermal insulating properties [16]. However, to the author’s best knowledge, the use of FAAMs as a high-performance insulation material with high mechanical resistance and low thermal conductivity has not been proven.

In this study, the potential of producing a high-performance FAAM made entirely from tungsten mining waste and municipal waste glass which could satisfy not only thermal performance but also mechanical strength requirements of similar grade products was

investigated. The compatibility of a natural foam catalyser and foam stabilising agent were investigated in order to improve both the thermal insulation and compressive strength performance. In addition, the preparation of a FAAM using mechanically pre-formed foam composed of an anionic surfactant and the alkali-activator, never reported in previous works, was studied.

2. Materials and Methods

2.1 Materials and chemicals

The precursor materials used to produce the FAAM in this investigation consisted of tungsten mining waste (TMW) and municipal waste glass (WG). The TMW was derived in powder form from the Panasqueira mine in Castelo Branco, Portugal, while the WG was received from the local municipality of Covilhã, Portugal. The micro-morphology of the TMW and WG can be seen in our previous study [22]. The chemical composition of TWM and WG from a sequential benchtop wavelength dispersive X-ray fluorescence (WD-XRF) spectrometer (Supermini200, Rigaku, Japan mounted with LiF(200) and PET crystals), is shown in Table 1. The raw materials used for the alkali activator were 98% pure sodium hydroxide (NaOH) (SH) (Fisher Scientific, Germany), and sodium silicate (Na_2SiO_3) (SS) (Solvay SA, Portugal).

Table 1. Chemical composition (wt %) of TMW and WG determined by WD-XRF

Component	TMW	WG
Na_2O	0.51	12.44
MgO	2.16	1.76
Al_2O_3	14.89	2.12
SiO_2	49.17	68.71
SO_3	8.98	0.33
K_2O	2.92	0.77
Fe_2O_3	13.69	1.48
CaO	0.58	10.04
P_2O_5	0.32	0.00
TiO_2	0.5	0.00
ZnO	1.25	0.00
CuO	0.32	0.00
As_2O_3	4.26	0.00

Foaming was achieved by either a chemical foaming technique or physical foaming technique. Aluminium powder (purity of 99 %, average particle size of 75 microns and molar mass of 26.98 g/mol, Sigma Aldrich, UK) was used as the foaming agent of the chemical foaming technique. Sodium dodecyl benzenesulfonate (SDBS, Sigma Aldrich, UK, molecular weight of 348.48 g/mol), was used for the physical foaming technique due to its ionic nature and thus enhanced foam stability compared to non-ionic surfactants [23].

Manganese dioxide (MnO_2, particle size of less than 10 microns and a molecular weight of 86.94 g/mol, Sigma Aldrich, UK) was used to catalyse the reaction of the chemical foaming process. Also, starch (Sigma-Aldrich, UK) which is a natural, high-polymeric carbohydrate was used to stabilise the chemical foaming process.

2.2 Methods

Firstly, essential parameters associated with the production of a FAAM were investigated, namely the curing temperature and dosage of Na_2O (mass ratio of total Na_2O in the activating solution to precursor). The optimum curing temperature and dosage of Na_2O in terms of density were used as benchmarks and carried forward to produce the reference sample for evaluating the effects of manganese dioxide and starch.

The mix parameters analysed through a laboratory experiment of 18 TMW-WG-FAAM samples were curing temperature (40˚C, 60˚C, 80˚C and 100˚C), dosage of Na_2O (3.1%, 3.3% and 3.5%), wt.% of aluminium powder (3, 6 and 9), wt.% surfactant (2, 4 and 6), wt.% MnO_2 (0.2, 0.4 and 0.6) and wt.% starch (2, 4 and 6).

All sample preparation was carried out in a laboratory maintained at 20°C. For the preparation of the non-foamed base TMW-WG-AAM, the synthesis conditions for achieving the highest strength and satisfactory workability were adopted based on previously published results [24]. The precursor consisted of TMW and WG with a mass ratio of 3:2. The alkali activating solution consisted of 10M sodium hydroxide solution (plus the sodium silicate concentration) and 8 wt.% of water. The mass ratio of the alkali activating solution and precursor was fixed at 0.22.

To determine the relationship between the various parameters and indicators, the horizontal x-axis presented the parameters, i.e. curing temperature, dosage of Na_2O (in %), foaming agent, manganese dioxide and starch contents, while the vertical y-axis' presented the average of the assessment indicators, i.e. compressive strength and density.

2.2.1 Chemical Foaming Method

The principle of chemical foaming with aluminium powder is based on the reaction between aluminium and SH to produce H_2 gas, which initiates the expansion of the system according to the following chemical reaction formula [25]:

$$2Al + 2NaOH + 6H_2O = 2NaAl(OH)_4 + 3H_2 \quad \text{(Eq. 1)}$$

The TMW and WG were dry-blended in a commercial mixer at 300 rpm for five minutes, forming the precursor materials. The alkali activating solution was slowly added to the precursor materials and then stirred for 2.5 minutes at 200 rpm, followed by 2.5 minutes at 500 rpm to form the AAM paste. The aluminium powder was subsequently added to the AAM by weight of sodium hydroxide and stirred for a further 1 minute at 350 rpm. Plastic 4 x 4 x 16 cm^3 molds were filled with the paste in two stages. The TMW-WG-FAAM was then left to rest until the foaming process was complete. The rest period depended on the quantity of aluminium powder and the dosage of Na_2O since different combinations produced different rates of expansion.

2.2.2 Mechanically Pre-Formed Foaming Method

The anionic surfactant and the alkali activating solution were combined together (Fig. 1a) and then mixed at 1200 rpm for 5 minutes to form the foamed alkali activating solution (Fig. 1b). TMW and WG were dry-blended in a commercial mixer at 300 rpm for 5 minutes, forming the precursor materials and the foamed alkali activating solution was mixed into the precursor at 300 rpm for 5 minutes (Fig 1c). Finally, Fig. 1d exhibits the fresh surfactant TMW-WG-FAAM immediately after mixing. A beater attachment was used for the mixing to allow more air to be entrapped into the TMW-WG-FAAM.

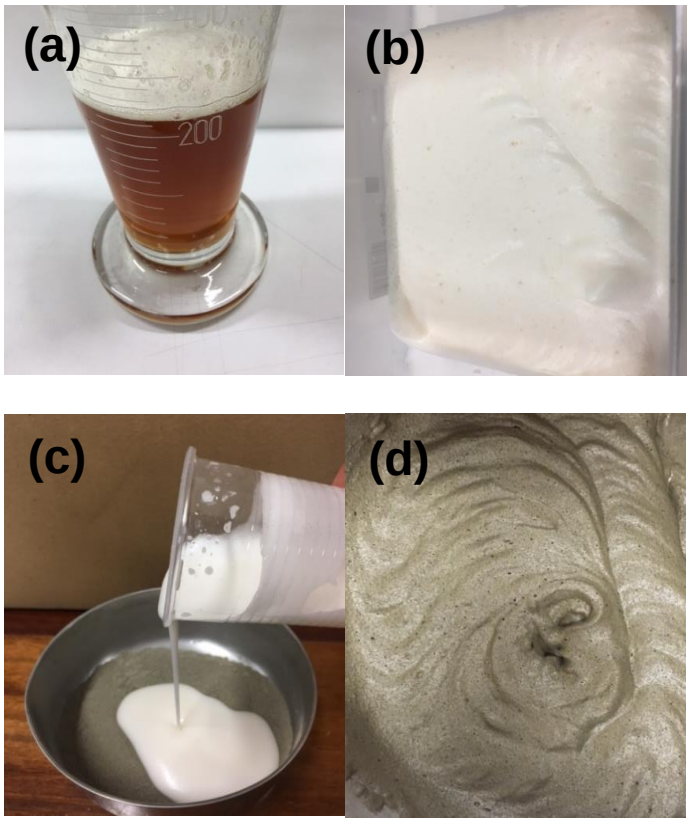

Fig. 1. Preparation of surfactant TMW-WG-FAAM showing (a) the alkali activator/surfactant mixture (b) prepared foam (c) combination of the precursors and foam (d) surfactant TMW-WG FAAM

2.2.3 FAAM Heat Curing Method

The specimens were placed in a temperature and humidity controlled environmental chamber at 95 %RH. The curing temperature was initially evaluated between 40°C and 100°C, with the most appropriate temperature in terms of compressive strength carried forward for the production of subsequent FAAM samples. After 24 hours of curing, the prismatic FAAM samples were demoulded and each of them was then cut into three 40 x 40 x 40 mm^3 cubes.

2.2.4 Thermal Conductivity

The thermal conductivity was measured with a thermal conductivity meter (Fox 200, TA Instruments, USA). The steady state heat flux through the 150 x 150 x 25 mm^3 rectangular block samples were measured for a temperature gradient of 10°C between the upper and the lower face of the sample. Three identical samples for each TMW-

WG-FAAM were measured for evaluation of the thermal conductivity. Before measurement, the samples were left for 12 h at 80°C and placed in a dry chamber for cooling for 30 minutes without moisture absorption.

2.2.5 Compressive Strength

The compressive strength of the TMW-WG-FAAM cubes was tested after 7 days in accordance with EN 196-1 using a 50kN universal testing machine (Instron 5960, UK) at a constant loading rate of 3 kN/min. The compressive strength value was the average of values obtained from three specimens.

2.2.6 Imaging

TMW-WG-FAAM samples were vacuum impregnated with epoxy resin doped with a fluorescent dye (EpoDye, Solvent Yellow 43, Denmark) to highlight the pores. The samples were polished using a bench-top planar grinding machine (PlanarMet 300, Buehler USA) and imaged using a fluorescence microscope (Leica M205 FCA, UK). Images were analysed using open source software (ImageJ) using a sample surface area of 22 x 22 mm.

3. Results and Discussion

3.1 TMW-WG FAAM by chemical foaming technique

3.1.1 Effect of heat curing

Fig. 2 shows the effect of curing temperature on the 7-day compressive strength and density of the TMW-WG-FAAM samples using 6% wt. of aluminium powder, a Na_2O of 3.1% and additional 8% wt. of mixing water. It is evident the compressive strength of the sample increased with curing temperature, while the density remained in practical terms unchanged within the range of 0.97 and 1.01 g/cm^3. As expected, the lowest compressive strength was attained by the sample cured at the lowest temperature (i.e. 40°C), reaching 3.15 MPa. Likewise, the compressive strength increased with increase in curing temperature due to the accelerated ion diffusion rate

between the liquid and solid material thus producing a denser colloidal structure [26]. TMW-WG-FAAM samples cured at the highest temperature, i.e. 100°C obtained a compressive strength of 5.45 MPa. The ultimate compressive strength and density of the samples were not found to be interdependent, and thus the optimal curing temperature of TMW-WG-FAAM may be based on a compromise of the compressive strength. In this case, the 80°C cured sample attained only a 4.6% lower compressive strength over the 100°C cured sample but consumed approximately 40 kWh less energy during curing (based on the energy performance of a Weiss C340-40 model environmental chamber operating for 24 hours). By considering the energy consumption during manufacturing, mechanical performance and thermal resistance, curing at 80°C was chosen to be the optimum curing temperature, in line with results obtained by other studies [27] and thus used for the preparation of all subsequent samples.

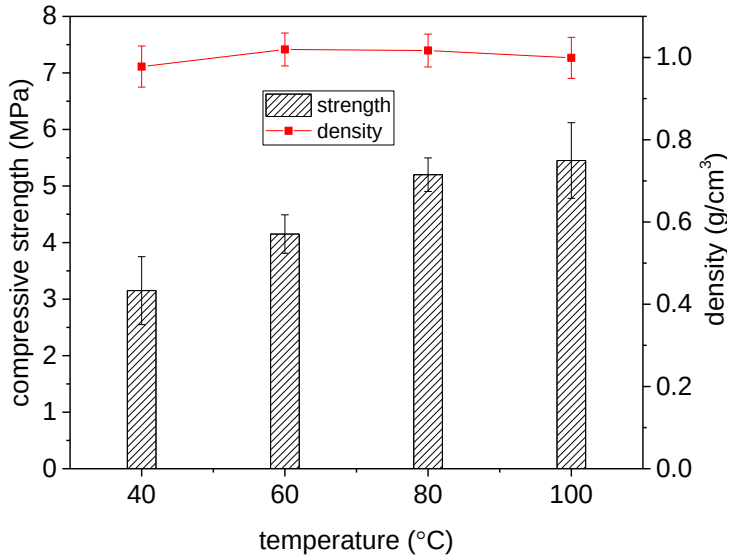

Fig. 2. Effect of curing temperature on compressive strength and density of aluminium powder TMW-WG FAAM

3.1.2 Effect of dosage of Na_2O

Fig. 3 demonstrates the effect of the 3.1%, 3.3% and 3.5% of Na_2O on the 7-day compressive strength and density of the TMW-WG-FAAM samples made using 6% wt. of aluminium powder and 8% wt. of mixing water. It was clear that the density of TMW-WG-FAAM reduced with increase of the %Na_2O. The formation of H_2 gas led to a foaming effect which would be enhanced with the increase of SH. Increasing the dosage of Na_2O from 3.1% to 3.5% reduced the density by 49% from 1.34 g/cm^3 to 0.67 g/cm^3. The increased foaming increased the porosity and reduced the density, but was naturally coupled by a reduction in the compressive strength of the TMW-WG-FAAM. In this case, the compressive strength reduced from 11.36 MPa to 3.3 MPa. Under normal circumstances, aluminium does not react with water, as an impermeable protective layer composed of aluminium hydroxide forms within seconds [25]. With the addition of sodium hydroxide, the aluminium hydroxide goes into solution, and the layer of aluminium oxide previously formed by passive corrosion is dissolved. For this reason, the alkali activating solution with a low Na_2O (less than 3.1%) involved a very slow reaction due to insufficient SH, leading to reduced volumetric expansion of the foam.

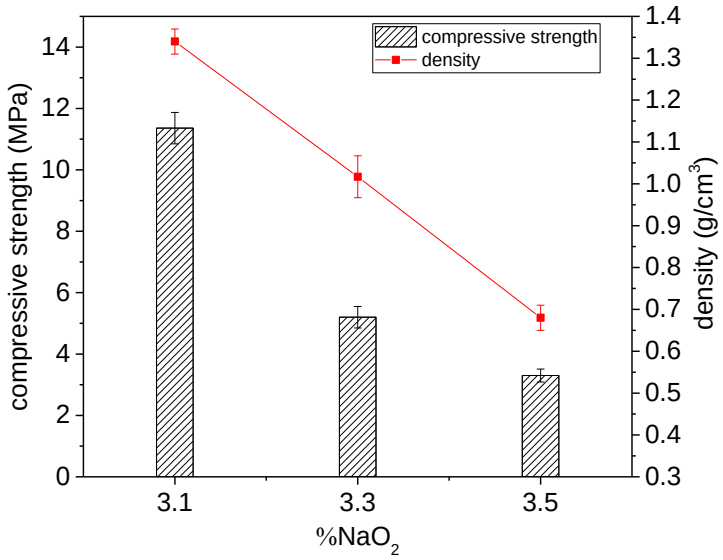

Fig. 3. Effect of %NaO_2 on compressive strength and density of aluminium powder AAFM

3.1.3 Effect of aluminium powder content

Fig. 4 shows the effect of 3% wt., 6% wt. and 9% wt. aluminium powder dosage on the 7-day compressive strength and density of the TMW-WG-FAAM sample made using dosage of Na_2O of 3.5% and 8% wt. mixing water. The sample density obtained with 3% wt. of aluminium powder was 1.52 g/cm^3, which went on to decrease to 0.68 g/cm^3 and 0.6 g/cm^3 for 6% wt. and 9% wt. aluminium powder dosages, respectively. The compressive strength also experienced a reduction by 67% from 9.2 MPa to 3 MPa, respectively. The reduction in compressive strength with increase in aluminium powder dosage was expected and due to the straightforward fact that more aluminium powder was available to react with the SH, producing more H_2 gas. Additionally, the high reaction rate between the aluminium powder and SH would have also led to the premature depletion of SH, reducing its availability for the required dissolution of aluminosilicate precursors; a factor known to interrupt the attainment of mechanical strength in AAMs [28]. It can also be deduced that the extent to which the foaming action and thus reduction in density occurs is less dominant with the increase of aluminium powder than with the increase of the alkali content i.e. %Na_2O. The latter

would make the alkali content and thus the appropriate optimisation of the activating solution the controlling factor in aluminium powder FAAMs.

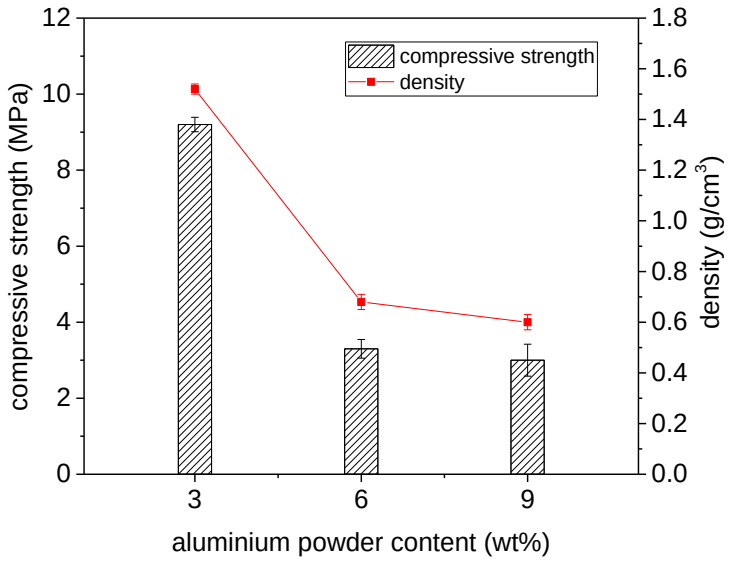

Fig. 4. Effect of aluminium powder on compressive strength and density of aluminium powder FAAM

3.1.4 Effect of manganese dioxide content

Fig. 5 compares the effect of 0.2% wt., 0.4% wt. and 0.6% wt. manganese dioxide catalysing agent dosage on the 7-day strength of TMW-WG-FAAM sample made using 6% wt. aluminium powder, 3.5% dosage of Na_2O and 8% wt. mixing water. With the initial presence of 0.2% wt. manganese dioxide, it is observed that the compressive strength of TMW-WG-FAAM significantly dropped by 61% from 3.3 MPa to 1.27 MPa. From 0.2 to 0.4 wt% and finally to 0.6 wt%, there appeared to be much steadier reduction in the density and compressive strength. The large initial drop and subsequent gradual reduction in density and thus compressive strength was due to the thermite reaction between the manganese dioxide and the aluminium powder foam. With the presence of manganese dioxide the foaming action was observed to be more unstable, resulting in excessive bubble size and their subsequent rupture. Therefore, it could be concluded that the incorporation of manganese dioxide should be avoided in aluminium powder FAAMs.

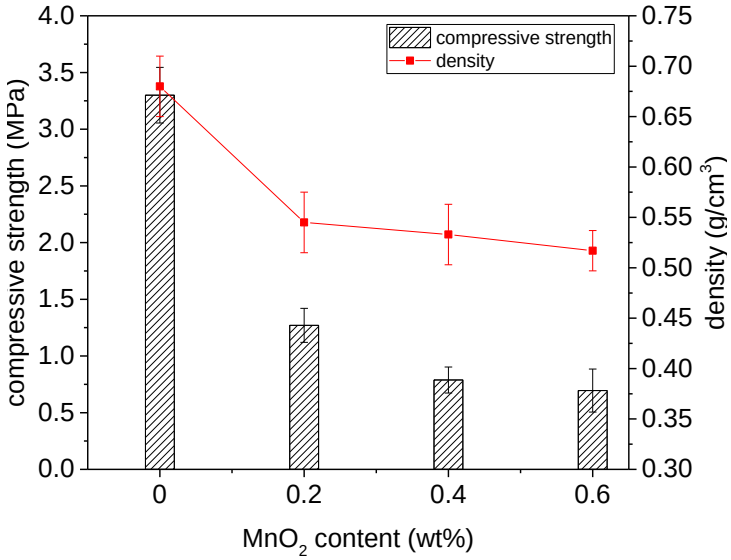

Fig. 5. Effect of manganese dioxide on compressive strength and density of 6% wt. aluminium powder TMW-WG FAAM

3.1.5 Effect of starch content

Fig. 6 shows the effect of 2% wt., 4% wt. and 6% wt. starch on the density and compressive strength of TMW-WG-FAAM made with 6 wt% aluminium powder, 3.5% Na_2O and 8 wt% mixing water. With the addition of 2% wt. starch, the density only marginally reduced from 0.68 g/cm^3 to 0.64 g/cm^3, while the compressive strength showed more noteworthy increase from 3.3 MPa to 3.8 MPa. This indicated that starch did not necessarily participate in the chemical foaming process but however improved the compressive strength. Starch being a polysaccharide was likely able to achieve this improvement in compressive strength due to its aggregating action in aluminosilicate interparticle bonds [29]. Nonetheless, when the starch concentration increased to 4% wt. and followed by 6% wt, the compressive strength significantly decreased, coupled by the increase in the density. The addition of starch above 2% wt. increased the relative concentration of particles in the system thus increasing the reaction time and subsequent formation of reaction products. The loss of compressive strength could be explained by the reduced liquid-solid ratio due to the low molecular weight of starch, resulting in a prolonged coagulation time of the FAAM and reduced

paste fluidity. The reduced fluidity due to the increased starch content created an open-textured material, and as revealed in Fig. 7, allowed the bubbles to coalesce (circled in black), and the H_2 gas generated during the aluminium powder and SH reaction to escape.

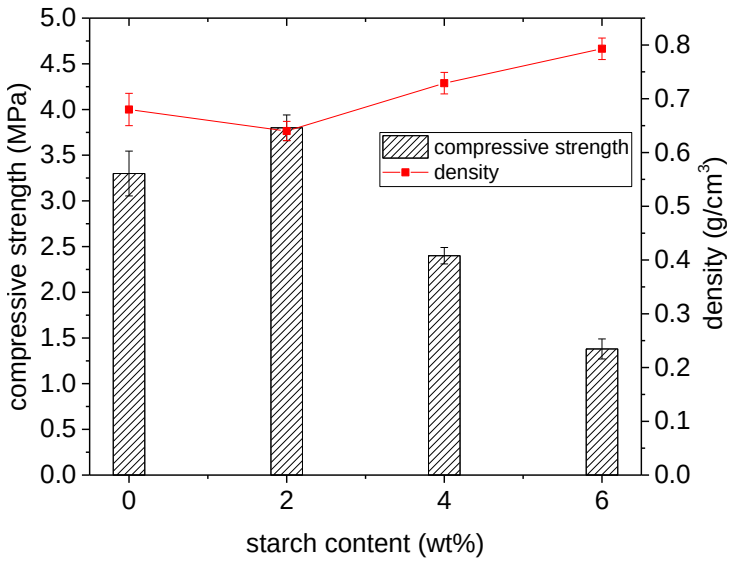

Fig. 6. Effect of starch on compressive strength and density of aluminium powder TMW-WG FAAM

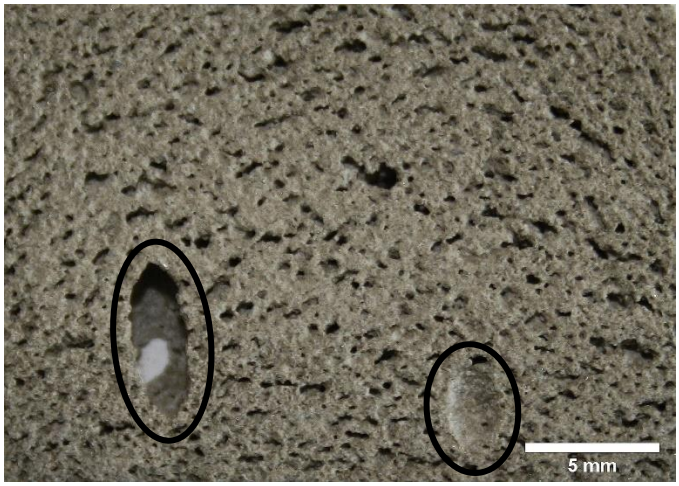

Fig. 7. TMW-WG FAAM made with 6% wt. starch

3.2 TMW-WG FAAM by physical foaming technique

2% wt., 4% wt and 6% wt. anionic surfactant were investigated in the preparation of the surfactant TMW-WG-FAAM. In all cases, the precursor-to-foam ratio was maintained at a constant ratio of 0.6.

3.2.1 Effect of surfactant content

Fig. 8 compares the effect of 2% wt., 4% wt and 6% wt. anionic surfactant on the compressive strength and density of the TMW-WG-FAAM samples made with 3.5% of Na_2O and 8 wt% mixing water. The compressive strength of the samples was observed to increase with an increase in the dosage of surfactant from 2% wt. to 4% wt. by 40% from 1.59 MPa to 2.68 MPa, respectively. However, the density remained steady between 0.71 and 0.75 g/cm^3. The increase in surfactant from 2% wt. to 4% wt. did not lead to an entrainment of more air in the sample thus explaining the approximately constant density. Upon the addition of 6% wt. surfactant, the density of the sample increased coupled by a reduction in the compressive strength. A likely explanation of the foaming inhibition with increased amounts of surfactant may be due to the presence of Ca^+ and Mg^+ ions from the precursor materials i.e. the TMW and WG which would have a strong affinity to the negatively charged carboxylate end of the surfactant molecule. This would essentially deactivate the surfactant and thus interrupt the foaming. Furthermore, increased surfactant content may have also led to an unnecessary high foam content, increasing the drainage of water around the foam thus increasing the likelihood of bubble collapse. However, further tests of increased surfactant content will have to be performed to confirm its impact on the compressive strength of TMW-WG-FAAM.

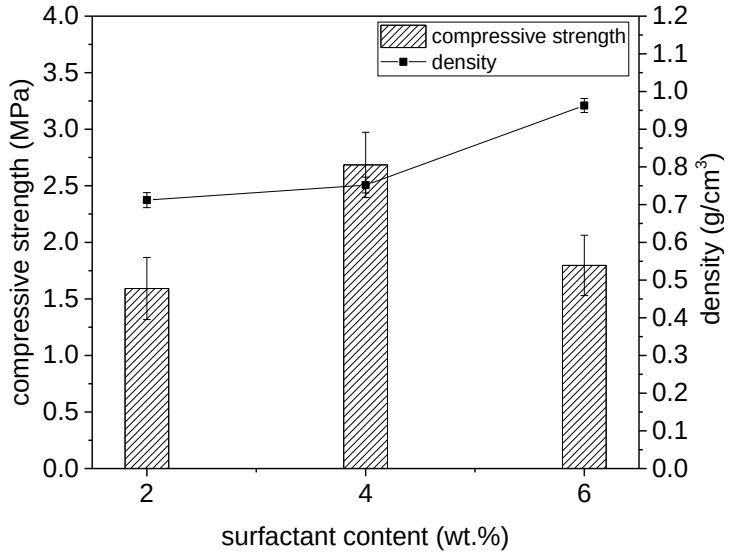

Fig. 8. Effect of surfactant on compressive strength and density of surfactant TMW-WG-FAAM

3.3 FAAM Pore Imaging and Thermal Conductivity

Grey level histogram analysis followed by a noise cleaning process were performed on medium magnification grey-scale surface images of TMW-WG-FAAM made with aluminium powder and surfactant. This procedure revealed clear outlines of all the pores and allowed for the calculation of their size by dividing the sum of their pixels by the total pixels in the image. Images of the deconvoluted TMW-WG-FAAM pore structures are presented in Fig. 9. TMW-WG-FAAM made by chemical foaming technique in Fig. 9a shows that most of the pore walls, or surfaces of the pores, are broken and interconnected, indicating that an open pore structure formed during foaming between the aluminium powder and SH. In comparison, most of the pores in TMW-WG-FAAM by physical foaming technique shown in Fig. 9b are spheroidal but possess little connectivity, indicating that the use of a surfactant as a foaming agent leads to a closed foam structure. Also, the average area of the pores TMW-WG-FAAM by physical foaming technique, calculated at 0.127 mm^2 (excluding the three large pores at the bottom right which are assumed to have formed during compaction) was 10% lower than the average pore size of the TMW-WG-FAAM by chemical foaming technique, calculated at 0.141 mm^2. It is the former open cell structure and larger

344 average pore size of the by chemical foaming technique which would allow for more
345 air to be trapped within the material, thus leading to a lower density and thus thermal
346 conductivity.
347 Using the images in Fig. 9a and 9b, a quantification of pore area distribution using the
348 variation of the pore area fraction along the depth of the specimens were also
349 performed. The images were divided into 2 mm deep x 22 mm wide strips, and the
350 pore area fractions in each of the strips were determined. The variation of pore area
351 shown in Fig. 9c corresponds to the average of pore area fraction measurements on
352 eleven different horizontal sections for TMW-WG FAAM foamed with aluminium
353 powder and surfactant. It can be noticed that there is a lower variation with depth in
354 the pore area fraction for the TMW-WG FAAM made with surfactant. The latter
355 indicates a more uniform distribution of pores across the TMW-WG FAAM made with
356 surfactant and corroborated with observations from Fig. 9b which show it to possess
357 more spherical and uniformly distributed pores. For the TMW-WG FAAM made with
358 aluminium powder, a higher degree of variation is observed through the image
359 analysis, implying a less stable foam structure and the possibility of foam clogging,
360 particularly at the top of the sample where the porosity was determined to be
361 approximately 18% less than at the bottom of the sample.

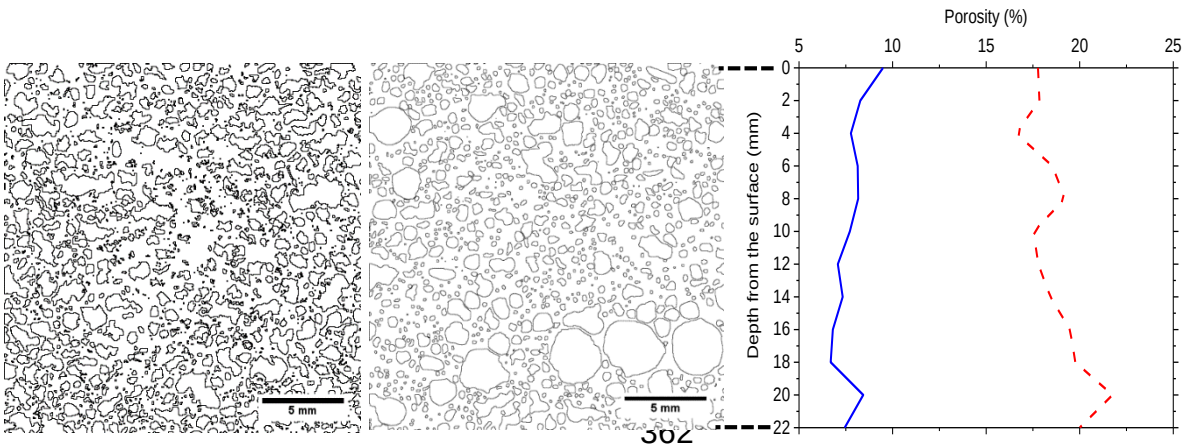

362

363 **Fig. 9.** (a) Pore distribution of TMW-WG FAAM foamed with (a) aluminium powder and (b) surfactant.
364 (c) Variation of pore area fraction in TMW-WG FAAM made with aluminium powder and surfactant.

Table 2 summarises the primary TMW-WG-FAAM properties, i.e. density, 7-day compressive strength and thermal conductivity for samples produced with the aluminium powder and surfactant foaming agents. Due to the open pore structure of TMW-WG-FAAM by chemical foaming technique, it is clear to understand why it achieved a lower density of 0.64 g/cm^3 and a thermal conductivity of 0.09 W/mK. The TMW-WG-FAAM by physical foaming technique achieved both a higher density and higher thermal conductivity of 0.77 g/cm^3 and 0.16 W/mK, respectively due to the closed pore structure and smaller average pore area. In practice, closed cell structures usually possess higher compressive strengths due to the higher core density but in the case of the open cell TMW-WG-FAAM by chemical foaming technique, it achieved a compressive strength of 3.8 MPa compared to the closed foam structure of the TMW-WG-FAAM by physical foaming technique of 2.68 MPa. This is an interesting observation and leads to the postulation that the chemical foaming technique is not only linked to pore characteristics such as shape and connectivity as previously mentioned, but also to its strength. In this case, the TMW-WG-FAAM by chemical foaming technique can be thought to have contributed to reinforcing the pore wall structure; however, this would require further investigation.

Table 2 also lists thermo-physical properties of traditional cement-based insulation materials and recently published foamed alkali-activated materials. By comparing between the best performing TMW-WG-FAAM reported in this study (prepared with 6 wt.% aluminium powder and 2% wt. starch) and other materials, the TMW-WG-FAAM significantly outperforms the traditional cement-based insulation materials such as AAC, foamed concrete and cement expanded vermiculite in terms of thermal conductivity while the combination of density and compressive strength is also unmatched.

391 **Table 2.** Thermo-physical properties of TMW-WG-FAAM, traditional cement-based insulation materials
392 and alkali activated foam materials

Sample	Density (g/cm^3)	Compressive strength (MPa)	Thermal conductivity (W/mK)
Unfoamed TMW-WG-AAM	2.10	61.0	0.280
6% wt. aluminium powder TMW-WG-FAAM with 2% wt. starch	0.64	3.8	0.090
4% wt. surfactant TMW-WG-FAAM	0.77	2.68	0.150
Aerated concrete (AAC) [30]	0.60	4.5	0.160
Foamed concrete [31]	0.60	5.2	0.165
'Inorganic foams' [30]	0.67	6.0	0.145
'Geopolymer foam concrete' [32]	0.60	1.3	0.470
'Geopolymer foam' [33]	0.58	4.4	0.158
'Porous fly ash-GP' [29]	0.56	1.23	0.107

393

394 **4 Conclusions**

395 This study revealed that alkali-activated foamed materials (FAAMs) based on tungsten
396 mining waste and waste glass could be successfully prepared by a chemical foaming
397 method using aluminium powder and a physical foaming method by using pre-formed
398 foam with an anionic surfactant. The following conclusions can be drawn from the
399 results of this work:

400 • The curing temperature of TMW-WG-FAAM influenced the mechanical strength
401 but did not affect the density. The final pore structure is formed during the initial
402 foaming process and thus curing temperature was chosen based on adequate
403 compressive strength development, which in this case was 80°C.

404 • The alkali content is strongly related to both the density and compressive
405 strength of TMW-WG-FAAM making it more of a dominant control factor
406 compared to the content of aluminium powder. A NaO_2 dosage lower than 3.1%

involves a very slow reaction due to insufficient NaOH, leading to a reduced volume of foaming.

- The chemical foaming method with aluminium powder resulted in the creation of an open cell pore structure leading to a significantly lower thermal conductivity and density, coupled with enhanced compressive strength.
- Use of manganese dioxide foam catalyst agent, even at relatively low levels (0.2% wt.), resulted in unstable chemical foaming with aluminium powder and compromised compressive strength. On the other hand, the use of starch as a foam stabilising agent led to improved compressive strengths without affecting the density.
- The combined technical and sustainable advantages of TMW-WG-FAAM make it a viable route to yield insulating materials comparable to both traditional cement-based insulation materials and other recently reported foamed alkali-activated materials.

Acknowledgement

Partial finance support from the European Commission Horizon 2020 MARIE Skłodowska- CURIE Research and Innovation Staff Exchange scheme through the grant 645696 (i.e. the REMINE project) is greatly acknowledged.

References

[1] R. K. Dhir, M. D. Newlands, and A. McCarthy, *Use of Foamed Concrete in Construction*. Thomas Telford Publishing, 2005.

[2] M. A. Mousa and N. Uddin, "Experimental and analytical study of carbon fiber-reinforced polymer (FRP)/ autoclaved aerated concrete (AAC) sandwich panels," *Eng. Struct.*, vol. 31, no. 10, pp. 2337–2344, 2009.

[3] W. A. Thanoon, M. S. Jaafar, M. R. A. Kadir, A. A. A. Ali, D. N. Trikha, and A. M. S. Najm, "Development of an innovative interlocking load bearing hollow block system in Malaysia," *Constr. Build. Mater.*, vol. 18, no. 6, pp. 445–454, 2004.

[4] Y. H. M. Amran, N. Farzadnia, and A. A. A. Ali, "Properties and applications of foamed concrete: a review," *Constr. Build. Mater.*, vol. 101, no. Part 1, pp. 990–1005, 2015.

[5] M. O'Grady, A. A. Lechowska, and A. M. Harte, "Quantification of heat losses through building envelope thermal bridges influenced by wind velocity using the outdoor infrared thermography technique," *Appl. Energy*, 2017.

[6] L. Shen, J. Haufe, and M. K. Patel, "Product overview and market projection of emerging bio-based plastics," 2009. [Online]. Available: https://goo.gl/5Qwvy3. [Accessed: 13-Nov-2017].

[7] J. Unwin, M. R. Coldwell, C. Keen, and J. J. McAlinden, "Airborne Emissions of Carcinogens and Respiratory Sensitizers during Thermal Processing of Plastics," *Ann. Occup. Hyg.*, vol. 57, no. 3, pp. 399–406, 2013.

[8] N. Pargana, M. D. Pinheiro, J. D. Silvestre, and J. de Brito, "Comparative environmental life cycle assessment of thermal insulation materials of buildings," *Energy Build.*, vol. 82, no. Supplement C, pp. 466–481, 2014.

[9] R. Baetens, B. P. Jelle, and A. Gustavsen, "Aerogel insulation for building applications: A state-of-the-art review," *Energy Build.*, vol. 43, no. 4, pp. 761–769, 2011.

[10] R. Baetens, B. P. Jelle, J. V. Thue, M. J. Tenpierik, S. Grynning, S. Uvsløkk, and A. Gustavsen, "Vacuum insulation panels for building applications: A review and beyond," *Energy Build.*, vol. 42, no. 2, pp. 147–172, 2010.

[11] N. Ismail, D. Ph, H. El-hassan, D. Ph, and M. Asce, "Development and Characterization of Fly Ash – Slag Blended Geopolymer Mortar and Lightweight Concrete," vol. 30, no. 4, pp. 1–14, 2018.

[12] G. Görhan and G. Kürklü, "The influence of the NaOH solution on the properties of the fly ash-based geopolymer mortar cured at different temperatures," *Compos. Part B Eng.*, vol. 58, pp. 371–377, 2014.

[13] H. Cheng-yong, L. Yun-ming, M. Mustafa, and A. Bakri, "Thermal Resistance Variations of Fly Ash Geopolymers : Foaming Responses," *Nat. Publ. Gr.*, no. February, pp. 1–11, 2017.

[14] P. Duxson, A. Fernández-Jiménez, J. L. Provis, G. C. Lukey, A. Palomo, and J. S. J. van Deventer, "Geopolymer technology: the current state of the art," *J. Mater. Sci.*, vol. 42, no. 9, pp. 2917–2933, 2007.

[15] N. Tenn, F. Allou, C. Petit, J. Absi, and S. Rossignol, "Formulation of new materials based on geopolymer binders and different road aggregates," *Ceram. Int.*, vol. 41, no. 4, pp. 5812–5820, May 2015.

[16] M. R. Wang, D. C. Jia, P. G. He, and Y. Zhou, "Influence of calcination temperature of kaolin on the structure and properties of final geopolymer," *Mater. Lett.*, vol. 64, no. 22, pp. 2551–2554, 2010.

[17] P. Duan, C. Yan, W. Zhou, and W. Luo, "Fresh properties, mechanical strength and microstructure of fly ash geopolymer paste reinforced with sawdust," *Constr. Build. Mater.*, vol. 111, no. Supplement C, pp. 600–610, 2016.

[18] M. Y. J. Liu, U. J. Alengaram, M. Z. Jumaat, and K. H. Mo, "Evaluation of thermal conductivity, mechanical and transport properties of lightweight aggregate foamed geopolymer concrete," *Energy Build.*, vol. 72, no. Supplement C, pp. 238–245, 2014.

[19] Z. Zhang, J. L. Provis, A. Reid, and H. Wang, "Mechanical, thermal insulation, thermal resistance and acoustic absorption properties of geopolymer foam concrete," *Cem. Concr. Compos.*, vol. 62, pp. 97–105, 2015.

[20] M. M. A. B. Abdullah, K. Hussin, M. Bnhussain, K. N. Ismail, Z. Yahya, and R. Abdul Razak, "Fly Ash-based Geopolymer Lightweight Concrete Using Foaming Agent," *Int. J. Mol. Sci.*, vol. 13, no. 6, pp. 7186–7198, 2012.

[21] J. Feng, R. Zhang, L. Gong, Y. Li, W. Cao, and X. Cheng, "Development of porous fly ash-based geopolymer with low thermal conductivity," *Mater. Des.*, vol. 65, pp. 529–533, 2015.

[22] G. Kastiukas, X. Zhou, and J. Castro-Gomes, "Development and optimisation of phase change material-impregnated lightweight aggregates for geopolymer composites made from aluminosilicate rich mud and milled glass powder," *Constr. Build. Mater.*, vol. 110, pp. 201–210, 2016.

[23] C. Stubenrauch and R. Von Klitzing, "Disjoining pressure in thin liquid foam and emulsion films — new concepts and perspectives," *J. Phys. Condens. Matter*, vol. 15, pp. 1197–1232, 2003.

[24] G. Kastiukas, X. Zhou, and J. P. Castro-Gomes, "Towards preparation conditions for the synthesis of alkali-activated binders using tungsten mining waste," *J. Mater. Civ. Eng.*, 2017.

[25] A. Hajimohammadi, T. Ngo, and P. Mendis, "How does aluminium foaming agent impact the geopolymer formation mechanism ?," *Cem. Concr. Compos.*, vol. 80, pp. 277–286, 2017.

[26] Sindhunata, J. S. J. van Deventer, G. C. Lukey, and H. Xu, "Effect of Curing Temperature and Silicate Concentration on Fly-Ash-Based Geopolymerization," *Ind. Eng. Chem. Res.*, vol. 45, no. 10, pp. 3559–3568, 2006.

[27] P. Rovnaník, "Effect of curing temperature on the development of hard structure of metakaolin-based geopolymer," *Constr. Build. Mater.*, vol. 24, no. 7, pp. 1176–1183, 2010.

[28] N. Neithalath, "Effects of activator characteristics on the reaction product formation in slag binders activated using alkali silicate powder and NaOH," *Cem. Concr. Comp.*, vol. 34, p. 809, 2012.

[29] M. P. Seabra, J. A. Labrincha, R. M. Novais, L. H. Buruberri, and G. Ascens, "Porous biomass fl y ash-based geopolymers with tailored thermal conductivity," *Soil Sci. Soc. Am. J.*, vol. 55, pp. 1076–1080, 1991.

[30] P. Hlaváček, V. Šmilauer, F. Škvára, L. Kopecký, and R. Šulc, "Inorganic foams made from alkali-activated fly ash: Mechanical, chemical and physical properties," *J. Eur. Ceram. Soc.*, vol. 35, no. 2, pp. 703–709, 2015.

[31] W. She, Y. Chen, Y. Zhang, and M. R. Jones, "Characterization and simulation of microstructure and thermal properties of foamed concrete," *Constr. Build. Mater.*, vol. 47, pp. 1278–1291, 2013.

[32] R. A. Aguilar, O. B. Díaz, and J. I. E. García, "Lightweight concretes of activated metakaolin-fly ash binders, with blast furnace slag aggregates," *Constr. Build. Mater.*, vol. 24, no. 7, pp. 1166–1175, 2010.

[33] C. Bai and G. Franchin, "High-porosity geopolymer foams with tailored porosity for thermal insulation and wastewater treatment," *J. Mater. Res.*, vol. 32(17), pp. 3251–3259, 2017.